



Single Layered 4x4 Butler Matrix Without Phase-Shifters and Crossovers

Suleiman Aliyu Babale, Sharul Kamal Abdul Rahim, Oumar Alassane Barro,
Mohamed Himdi, Mohsen Khalily

► To cite this version:

Suleiman Aliyu Babale, Sharul Kamal Abdul Rahim, Oumar Alassane Barro, Mohamed Himdi, Mohsen Khalily. Single Layered 4x4 Butler Matrix Without Phase-Shifters and Crossovers. IEEE Access, 2018, 6, pp.77289-77298. 10.1109/ACCESS.2018.2881605 . hal-01987948

HAL Id: hal-01987948

<https://univ-rennes.hal.science/hal-01987948>

Submitted on 17 Jul 2019

HAL is a multi-disciplinary open access archive for the deposit and dissemination of scientific research documents, whether they are published or not. The documents may come from teaching and research institutions in France or abroad, or from public or private research centers.

L'archive ouverte pluridisciplinaire **HAL**, est destinée au dépôt et à la diffusion de documents scientifiques de niveau recherche, publiés ou non, émanant des établissements d'enseignement et de recherche français ou étrangers, des laboratoires publics ou privés.



Distributed under a Creative Commons Attribution 4.0 International License

Received October 21, 2018, accepted November 10, 2018, date of publication November 15, 2018, date of current version December 31, 2018.

Digital Object Identifier 10.1109/ACCESS.2018.2881605

Single Layered 4×4 Butler Matrix Without Phase-Shifters and Crossovers

SULEIMAN ALIYU BABALE^{1,2}, (Student Member, IEEE),
SHARUL KAMAL ABDUL RAHIM¹, (Senior Member, IEEE),
OUMAR ALASSANE BARRO³, MOHAMED HIMDI³,
AND MOHSEN KHALILY^{1,4}, (Senior Member, IEEE)

¹Wireless Communication Centre, Faculty of Electrical Engineering, Universiti Teknologi Malaysia, Skudai 81310, Malaysia

²Department of Electrical Engineering, Faculty of Engineering, Bayero University Kano, Kano 700241, Nigeria

³Institute of Electronics and Telecommunications of Rennes, University of Rennes1, 35042 Rennes, France

⁴Home of 5G Innovation Centre, Institute for Communication Systems, University of Surrey, Guildford GU2 7XH, U.K.

Corresponding author: Mohsen Khalily (m.khalily@surrey.ac.uk)

This work was supported in part by the Ministry of Higher Education Malaysia, Universiti Teknologi Malaysia, under Grant 4J213, and in part by the Institute of Electronics and Telecommunications of Rennes, University of Rennes1, France.

ABSTRACT Traditional design of 4×4 Butler matrix (BM) uses couplers, phase shifters (PSs), and crossovers. Due to some troublesome issues related to PS and the crossovers involved in the design of BM, which degrades its performance, this paper presents a planar 4×4 BM without PS and crossovers. It is accomplished with the help of a modified coupler. The modified coupler is realized to have a 45° output phase difference, which replaces the function of the 45° PSs. The 45° output phase differences obtained from this type of coupler combined with quadrature coupler give the desired phase differences required at the output of the BM. The BM is meant to operate at 6 GHz. The simulated and measured reflection coefficients and isolations at all ports are below -17 dB at the center frequency. The result also shows an amplitude imbalance within ± 3 dB with phase mismatch of about $\pm 3^\circ$ at the center frequency. The -10 -dB reflection coefficient bandwidth is 37.10%, and the transmission bandwidth between -5 and -9 dB is about 31.0%. Both the simulated and experimental radiation patterns obtained by exciting the input ports (P1–P4) of the BM produce four orthogonal beams deposited at $+15.3^\circ$, -47.6° , $+47.6^\circ$, and -15.3° . This beam steering depicts a stable beam scanning angle of the BM, which is in good agreement with the theoretical predictions.

INDEX TERMS Crossovers, Butler matrix, modified coupler and phase shifters.

I. INTRODUCTION

Due to the increase in number of subscribers and the need for high data rate in wireless communication systems, the demands for increase in channel capacity, mitigation of multi-path fading, and co-channel interference are paramount for mobile and satellite communication systems [1]. As the number of users increase, the co-channel interference also increases and led to inferior Quality of Service (QoS) [2]. This has triggered a lot of research in the area of beamforming network with the aim of tackling this problem and improve the quality of communication link even in uncomplimentary conditions.

The application of switched beam forming network (SBN) has been widely studied by researchers [3]–[6] and the technology was extensively being utilized in application related to

wireless communications. There are several type SBN, such as Blass matrix [7], Rotman lens [8], Nolen matrix [9] and Butler matrix (BM) [10]. The famous among the techniques is the BM due to its relatively simple configuration and low power dissipation [11]. Moreover, by taking advantage of its beam orthogonality, which gives it the capability of transmitting and receiving multiple beams concurrently, its beam scanning coverage and the channel capacity significantly improved [12].

The block diagram of conventional BM shown in Fig. 1 comprises of four couplers, two phase shifters and two crossovers. Phase Shifters (PS) and crossovers being part of the building block of the BM. The PS impairs the performance of the BM by introducing imbalance insertion losses [13] and unacceptable phase ripples due to edge-coupling of the

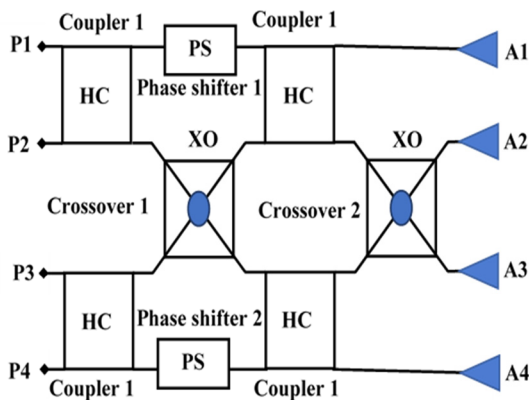


FIGURE 1. Block diagram of a conventional 4×4 Butler matrix.

lines [14]. Even though this problem can be minimized by modifying the ground plane of the coupled line structure as proposed by [15], the performance is still critically affected by errors due to fabrication.

However, from the crossover point of view, the conventional design suffers from narrow bandwidth and large electrical size due to the quarter wavelength requirements of the transmission-line sections [16]. Also, involving a cross-over points in a PCB layout requires additional photo mask step, which brings additional cost and complexity of the system. Furthermore, this will increase the risk of signal loss and unavoidable reflections due to parasitic capacitance and resistances present at the cross-over point that might seriously affect the system's performance. Underpasses, air bridges or bonding wires are sometimes used as an alternative to achieve crossing. However, these types of crossovers are nonplanar; thus, they increase the complexity of the design and results in excessive cost of fabrications [17].

Because of these inherent problems of PS and crossovers, [18] and [19] proposed BM without crossovers. But the multi-layer technique requires the use of vias which increase the fabrication difficulties. Reference [20] presented a BM without PS. But, unlike in the classical design of couplers, the patch hybrid coupler used cannot be characterized using simple closed-form transmission line theory due to the complicated nature of the field distribution on the cross-slot patches [21]. Similarly, some variables like the length, width, stubs, location of the concaves and the ground plane pattern has to be determined using complex and time-consuming optimization methods [22].

Most of the compact design of BM using microstrip transmission line concentrate on either miniaturizing size of the BM by already known methods like transforming the quarter wavelength into π or T , elimination of crossover points by means of multi-layered or elimination of only phase shifters as proposed in [20]. To the best of our knowledge, none of the research proposes a single-layered design of BM using microstrip technique by means of eliminating both the PS and crossovers. This paper proposes to design a novel single layered 4×4 planar BM using 3dB couplers only. The design utilizes modified hybrid couplers having

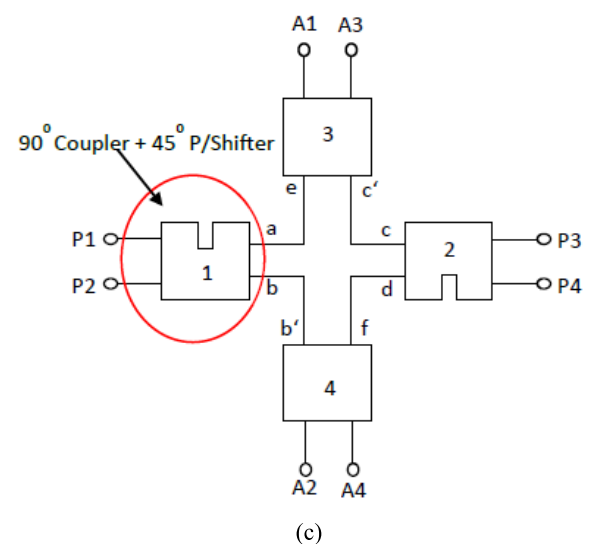
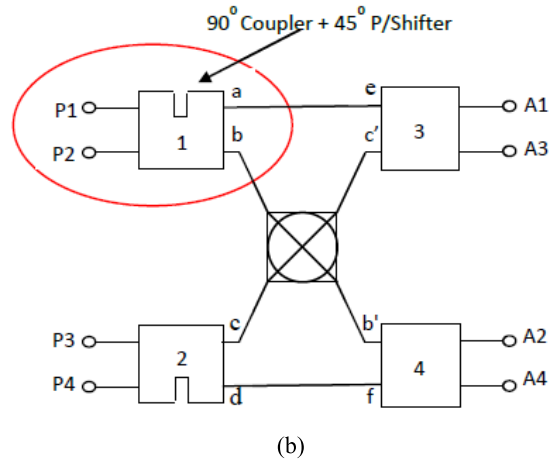
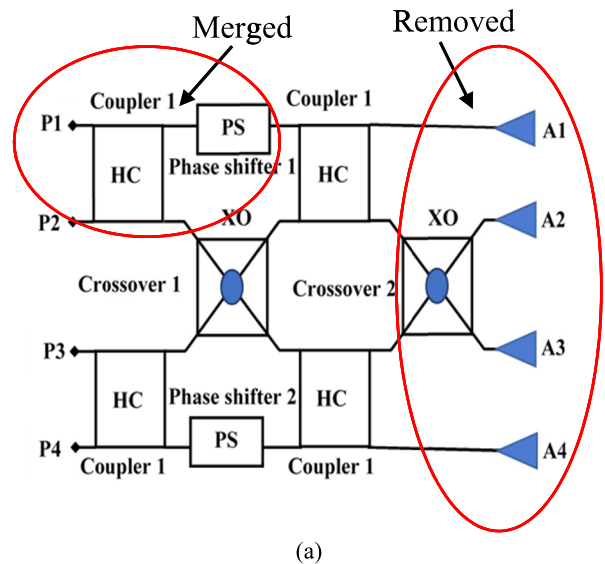


FIGURE 2. (a) Conventional BM merging and removing some of the crossovers; (b) simplified diagram a BM; (c) block diagram of the proposed 4×4 BM.

45° phase-difference as a replacement of the two quadrature couplers in building the BM as shown in Fig. 2(a).

Also, the topology used ensured total elimination of the phase shifters and therefore avoid any cross-over points in designing the proposed BM. From the input side of the BM, P1, P2, P3, and P4 are the input ports where a signal can be injected into the device. whereas, A1, A2, A3, and A4 represent the output antennas where either could be the radiating element depending on the input port selected.

The paper is organized in the following manner. Introduction was given in section I. Section II deals with detailed design concept using transmission line theory. In section III, the design procedures of the conventional and the modified couplers are presented, while the BM was designed and Implemented in Section IV. Finally, the concluding remarks are given in Section V.

II. DESIGN THEORY

The proposed BM shown in Fig. 2(c) was obtained as a result of simplifying the conventional BM of Fig. 2(a) by removing the output crossover, merging the quadrature coupler and the 45° PS. This simplified the structure to form a BM shown in Fig. 2(b) which produces 135°/45° phase-difference at point 'ab' that replaces the combination of the quadrature (90°) couplers and the 45° phase-shifters. Replacing these two components with the modified coupler gives the same effect as that produce by conventional design. Having successfully simplified the design, the nodes of the complete BM marked 'a' to 'f' in Fig. 2(b) are further simplified by mapping the various nodes in order to remove the crossover point as shown in Fig. 2(c). The design concept for the modified coupler 45° coupler was adapted from [23] with little modification that involved variable power and to accommodate the design of couplers having output phase difference up to 180° like rate race couplers. The design equations of the couplers are derived, and the resulting closed-form equations are used to design the both the conventional and the modified couplers. The schematic diagram of the proposed coupler is illustrated in Fig. 3.

Where Z_1 , Z_2 and Z_3 are the impedance of the main line and the branch of the coupler. The electrical lengths θ_1 , θ_2 and θ_3 represent the electrical length of the main line and the branches. The impedances Z_2 and Z_3 are assumed to be equal for simplicity. Port 1 is choosing as the input, port 2 and 3 are taken as the output ports, whereas port 4 remains the isolated port. Due to symmetrical nature of the coupler, it was divided into two horizontal segments for the analysis. Even-odd mode analysis was used to obtain the coupler parameters. Fig. 3(b) shows the even and odd mode equivalent circuit of the proposed coupler. The design criteria were aimed at achieving a variable phase difference, $\psi(f)$ and variable power division $P(f)$. The power division ratio and the phase difference between the output ports are defined as:

$$P(f)^2 = \left| \frac{S_{21}}{S_{31}} \right|^2 \quad (1)$$

$$\psi(f) = \angle S_{21} - \angle S_{31} \quad (2)$$

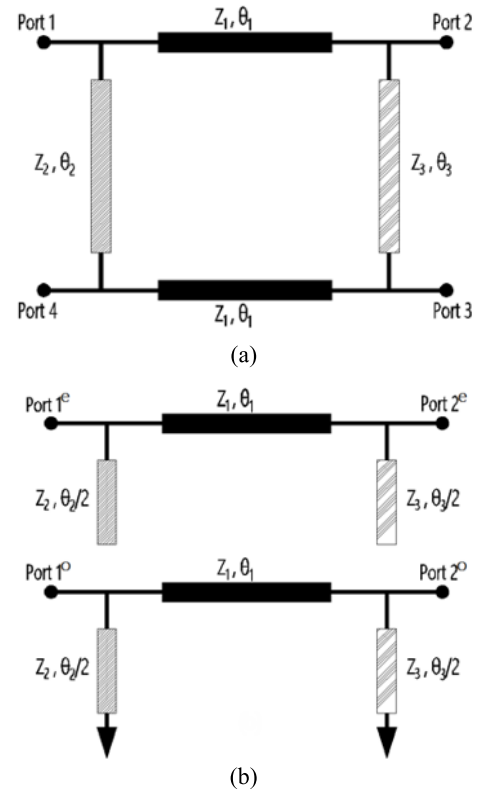


FIGURE 3. (a) Schematic representation of the proposed coupler; (b) even-odd mode representation.

From Fig. 3(b), the transmission characteristics of the even or odd mode is obtained using (ABCD) matrix, the overall transmission and reflection characteristics of the network is computed from the product of the matrices representing the individual sub-circuits of the even and odd circuits representation of the coupler.

$$\begin{bmatrix} A & B \\ C & D \end{bmatrix} = [T_a][T_b][T_a] \quad (3)$$

For the even-mode excitation, the ABCD parameters are as following:

$$\begin{bmatrix} A & B \\ C & D \end{bmatrix}_e = \begin{bmatrix} 1 & 0 \\ \tan\left(\frac{\theta_1}{2}\right)/Z_1^e & 1 \end{bmatrix} * \begin{bmatrix} \cos \theta_2 & jZ_2^e \sin \theta_2 \\ j \sin \theta_2 / Z_2^e & \cos \theta_2 \end{bmatrix} \times \begin{bmatrix} 1 & 0 \\ \tan\left(\frac{\theta_1}{2}\right)/Z_1^e & 1 \end{bmatrix} \quad (4)$$

where the superscript 'e' represents the even mode excitation. Multiplying and simplifying equation (4) gives the elements of the ABCD parameter as follows:

$$A_e = \cos \theta_2 - \left(Z_2^e \tan\left(\frac{\theta_1}{2}\right) \right) * \frac{\sin \theta_2}{Z_1^e} \quad (5)$$

$$B_e = (Z_2^e \sin \theta_2) i \quad (6)$$

$$C_e = (\sin \theta_2 / Z_2^e) i + (2 \tan\left(\frac{\theta_1}{2}\right) \cos \theta_2) i / Z_1^e$$

$$- \frac{Z_2^e \tan^2 \left(\frac{\theta_1}{2} \right) \sin \theta_2}{(Z_1^e)^2} i \quad (7)$$

$$D_e = \cos \theta_2 - \left(Z_2^e \tan \left(\frac{\theta_1}{2} \right) \right) * \frac{\sin \theta_2}{Z_1^e} \quad (8)$$

For the odd mode, the elements can be obtained in similar way to that of even mode with the parameters, $Y_1^o = -j \cot(\theta_1/\theta_2) / Z_1^o$ where the superscript 'o' stands for the odd mode excitation. Similarly, due to symmetry of the coupler, the elements A and D are equal for the even and the odd modes. However, the matrix elements B and C for the even mode are equal but with opposite sign to those of odd mode [24].

$$A_o = A_e \quad (9)$$

$$D_o = D_e \quad (10)$$

$$B_o = -B_e = - (Z_2^e \sin \theta_2) i \quad (11)$$

$$C_o = -C_e = + \frac{Z_2^e \tan^2 \left(\frac{\theta_1}{2} \right) \sin \theta_2}{(Z_1^e)^2} i - (\sin \theta_2 / Z_2^e) i - (2 \tan \left(\frac{\theta_1}{2} \right) \cos \theta_2) i / Z_1^e \quad (12)$$

The ABCD parameter obtained from the even-odd mode analysis are then converted to scattering parameter (S-parameter) with the help of an expression for reflection and transmission coefficients defined as [24]:

$$\Gamma = \frac{A + \frac{B}{Z_0} - CZ_0 - D}{A + \frac{B}{Z_0} + CZ_0 + D} \quad (13)$$

$$T = \frac{2}{A + \frac{B}{Z_0} + CZ_0 + D} \quad (14)$$

where Γ and T are the reflection and transmission coefficient of the system when signal is injected from the input port to the output. From the expressions of reflection coefficient Γ and transmission coefficient T , the scattering parameter can be obtained from [24]. Using (1)–(14) and applying perfect isolation and matching conditions on the S-parameter, the following simplified equations emerged:

$$Z_1 = Z_0 P |\sin \psi| \quad (15)$$

$$Z_2 = Z_3 = \frac{Z_0 P \sin \psi}{\sqrt{1 + P^2 \sin^2 \psi}} \quad (16)$$

$$\theta_1 = \frac{\pi}{2} \quad (17)$$

$$\theta_2 = \tan^{-1} \left(\frac{(Z_0 \tan \psi)}{Z_1} \right) \quad (18)$$

$$\theta_3 = \pi - \tan^{-1} \left(\frac{(Z_0 \tan \psi)}{Z_1} \right) \quad (19)$$

where, ψ is the phase difference at the center frequency and P^2 is the power division ratio of the coupler.

III. COUPLER DESIGN

Two types of couplers are used to accomplish the design of the proposed BM. These couplers are the conventional Quadrature coupler with output phase difference of 90° and a modified coupler whose output phase difference is 45°.

A. QUADRATURE COUPLER

Quadrature coupler is a four-port symmetrical network such that when any port of the coupler is fed with power, it is capable of dividing the power equally between the two opposite ports with 90° phase shift between these outputs while the adjacent port to the input is being completely isolated [25].

Using the designed equations (15) and (16), the impedances of the 3dB quadrature coupler were computed by setting the outputs phase difference $\psi = 90^\circ$ and the reference impedance $Z_0 = 50\Omega$, the impedances of the couplers' vertical and horizontal arms are: $Z_1 = Z_0 = 50\Omega$ and $Z_2 = Z_3 = 35.36\Omega$. With $Z_1 = Z_0$, equation (18) can be simplified as:

$$\theta_2 = \tan^{-1} (\tan \psi) = \psi \quad (20)$$

TABLE 1. Optimized parameters of the BLC.

Parameters	Values
Z1	35.36 (Ω)
Z2	50.00 (Ω)
θ ₁	90°
θ ₂	90°
θ ₃	90°
AL1	7.697 (mm)
AW1	1.102 (mm)
BL1	10.499 (mm)
BW1	0.678 (mm)
PL1	2.000 (mm)
PL2	3.449 (mm)
PL3	5.620 (mm)
PW1	0.667 (mm)

From (20), for a given the output phase difference of quadrature coupler as 90°, the electrical lengths of the coupler are $\theta_2 = \theta_3 = 90^\circ$. Table 1 shows the impedances and the optimized parameters of the coupler. The parameters of each sections are indicated on the layout of Fig. 4(a).

Having obtained good return loss, transmission coefficients and the output phase difference, the coupler was fabricated, measured and the photograph of the device under test is shown in Fig. 5(a).

The simulated and the measured results of the coupler are shown in Fig. 5. From this graph, the 10 dB fractional bandwidth was found to be from 4.93 GHz to 7.24 GHz which stands for about 38.50%. Furthermore, the bandwidth

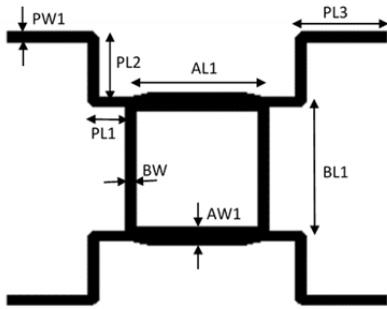


FIGURE 4. Layout of the quadrature coupler.

corresponds to the coupling of $-3 \text{ dB} \pm 1 \text{ dB}$ range from 5.29 GHz to 6.95 GHz, which translates to about 27.67%. Also, the measured output phases difference was found to be 90.14° . Considering a phase mismatch of less than $\pm 5^\circ$, the operational bandwidth was 32.17%.

B. MODIFIED COUPLER

The design of a 3dB modified coupler with outputs phase difference of 45° was accomplished by applying (15)–(20) to determine the various Impedances of the coupler arms. By setting the outputs phase difference ψ as 45° and the reference impedance Z_0 as 50Ω , with equal power division ratio, $p = 1$, the impedances of the coupler arms are obtained, and the optimized parameters are shown in Table 2.

TABLE 2. Optimized parameters of the proposed coupler.

Parameters	Values
Z1	35.36 (Ω)
Z2, Z3	28.87 (Ω)
θ_1	90°
θ_2	120°
θ_3	60°
AL1	5.634 (mm)
AW1	1.084 (mm)
BL1	9.413 (mm)
BW1	0.925 (mm)
PL1	2.662 (mm)
PL2	3.886 (mm)
PL3	5.867 (mm)
PW1	0.667 (mm)
L1	2.492 (mm)
L2	4.750 (mm)
L3	2.817 (mm)
W	1.084 (mm)

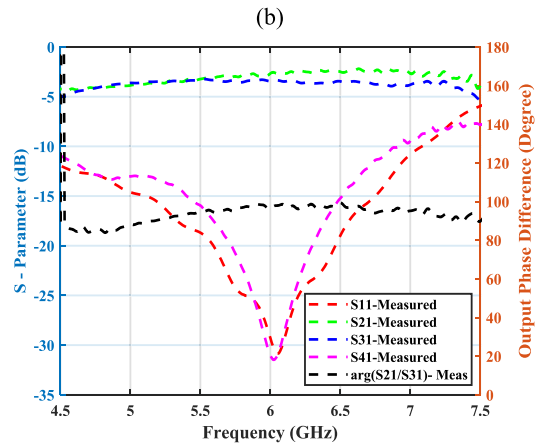
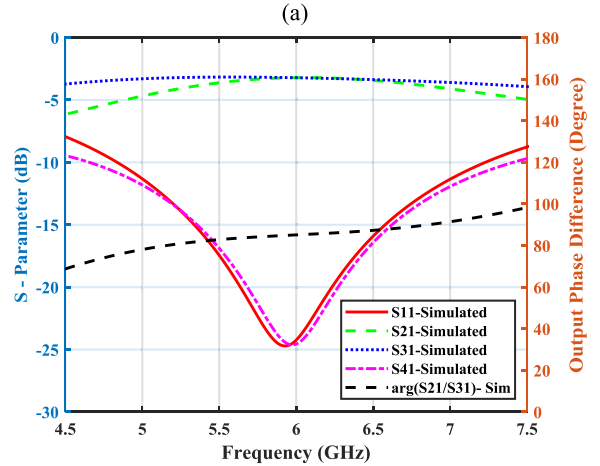
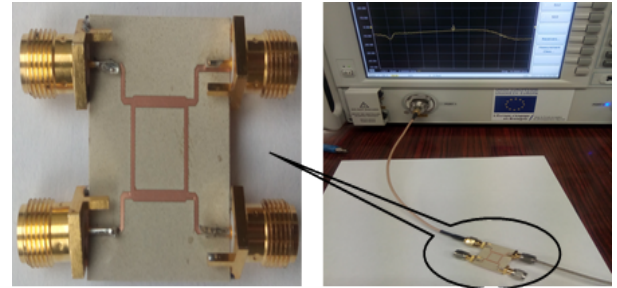


FIGURE 5. (a) Photograph of the quadrature coupler under test. (b) Simulated S-Parameter results of the quadrature coupler. (c) Measured S-Parameter results of the quadrature coupler.

Similarly, the optimized parameters of each section of the modified coupler are indicated on the layout shown in Fig. 6.

Fig. 7 shows the photograph of the fabricated coupler and the S-parameter showing the reflection coefficient, transmission coefficients and the output phase difference.

From these plots, the measured S_{11} and S_{41} coincide at -23.88 dB whereas, S_{21} , and S_{31} are -3.13 dB and -3.34 dB and the output phase difference is 45.23° at 6 GHz. The bandwidth achieved for this phase difference with imbalance less than $\pm 5^\circ$ was found to be from 5.19 GHz to 7.01 GHz, which corresponds to 30.2%.

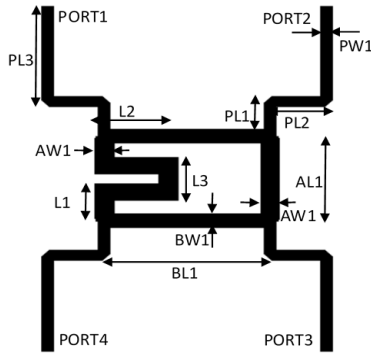


FIGURE 6. Layout of the modified coupler.

IV. BUTLETR MATRIX DESIGN

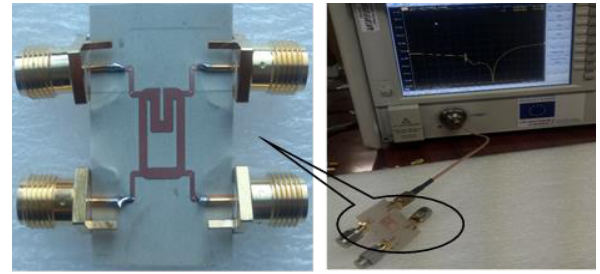
The proposed BM was designed completely from the conventional and the proposed couplers designed in the previous section, without using any additional component. A commercially available, Computer Simulation Technology (CST) was used throughout the simulation and the prototype was manufactured using laser machine with Rogers' substrate RO3003, whose dielectric constant is 3.0, loss tangent of 0.027 and a thickness of 0.25mm.

The circuit layout and the photograph of the fabricated BM are shown in Fig. 8. When any input Port of a BM is fed with signal, it splits equally among the four output ports with coefficients of transmission within the around -6 dB and a return loss better than -10 dB across the bandwidth.

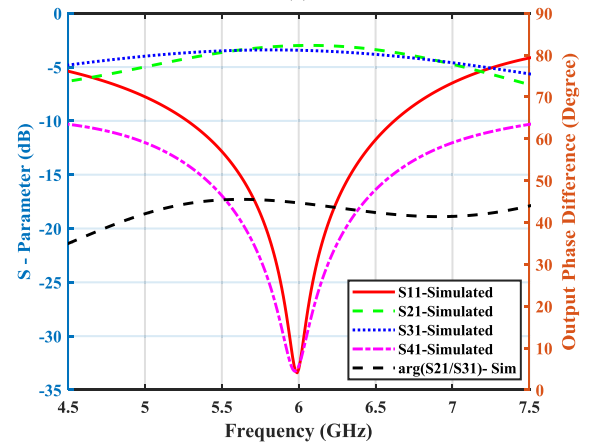
Vector Network Analyzer (N5222A) from Keysight Technologies, capable of measuring a device working from 10 MHz up to 29.5 GHz was used to obtain the measured S-parameter results of the fabricated BM. Fig. 9 shows the Photograph of the Device Under Test (DUT) using the VNA after calibrated with calibration kit 85052D. During the measurements, all the unused ports were terminated with 50 ohms load.

The simulated and measured S-parameter results showing the return losses and transmission coefficients at various ports are shown in Fig. 10. Due to the symmetrical nature of the device, when a signal is injected into port 1 (similar to port 4) of the BM, the return loss obtained from the simulation and the measurement were -27.41 dB and -24.75 dB respectively. Also, the measured transmission characteristics are $S_{51} = -7.94$ dB, $S_{61} = -8.32$ dB, $S_{71} = -7.59$ dB, and $S_{81} = -7.05$ dB at the operating frequency. Similarly, when port 2 (similar to port 3) is exited, the measured $S_{22} = -24.24$ dB and the transmission coefficients are $S_{52} = -7.45$ dB, $S_{62} = -7.22$ dB, $S_{72} = -8.01$ dB, and $S_{82} = -8.56$ dB at the center frequency. In both cases, the transmission coefficients are close to the theoretical value of -6 dB with slight discrepancy of about ± 3 dB.

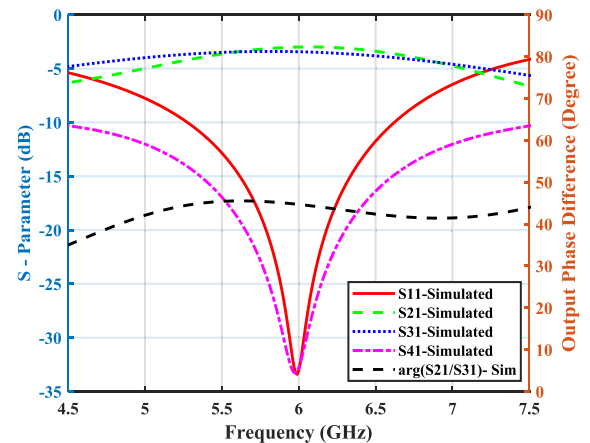
To ensure that the BM satisfy the required progressive phase differences in accordance to the theoretical values, the progressive phase difference was plotted as shown in Fig. 11. From this Figure, the differential output phases obtained by exciting Port 1, port 2, port 3 and port 4 at



(a)



(b)

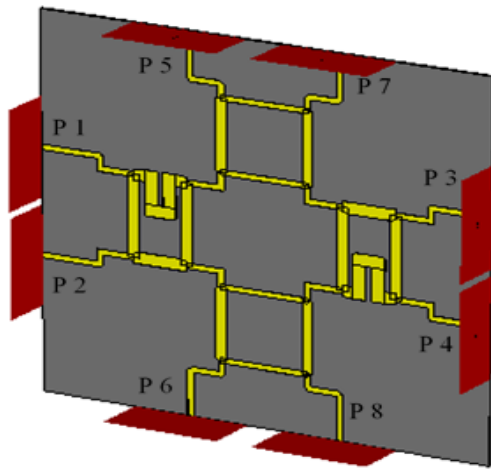


(c)

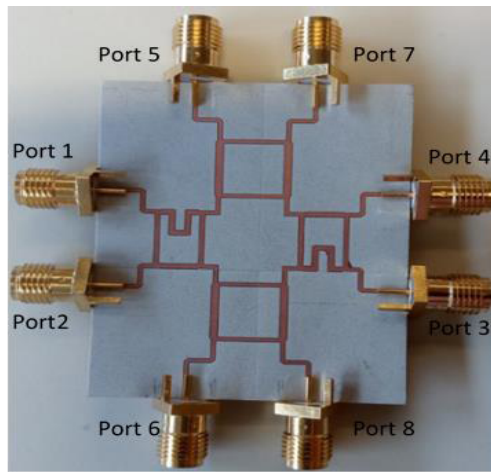
FIGURE 7. (a) Photograph of the modified coupler under test. (b) Simulated S-Parameter results of the modified coupler. (c) Measured S-Parameter results of the modified coupler.

the center frequency are $+45^\circ$, -135° , $+135^\circ$ and -45° respectively.

When antenna array is connected to the output ports and excite any of the input while terminating the remaining ports with the line characteristic impedance (usually 50Ω), four different progressive-phase distribution responses are produced each pointing in the directions of $\pm 14.5^\circ$ and $\pm 48^\circ$. These responses have equal amplitude and progressive phase differences designated by β . Being symmetrical device, the value of β resulting by exiting any of the input ports is either $\pm 45^\circ$ or $\pm 135^\circ$. The radiation characteristic of the



(a)



(b)

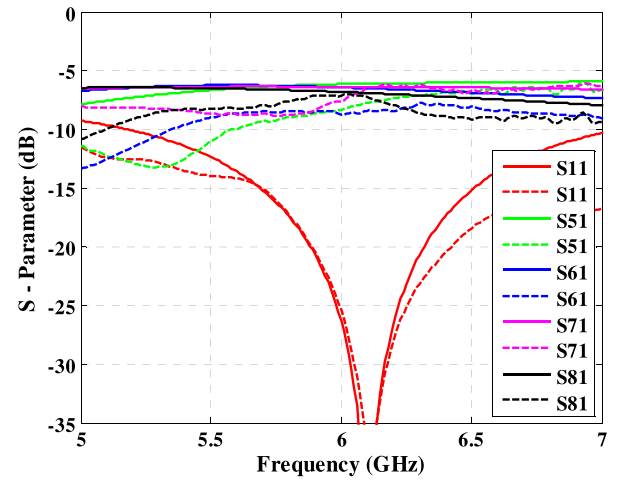
FIGURE 8. The proposed Butler matrix (a) layout, (b) photograph of the fabricated Butler matrix.



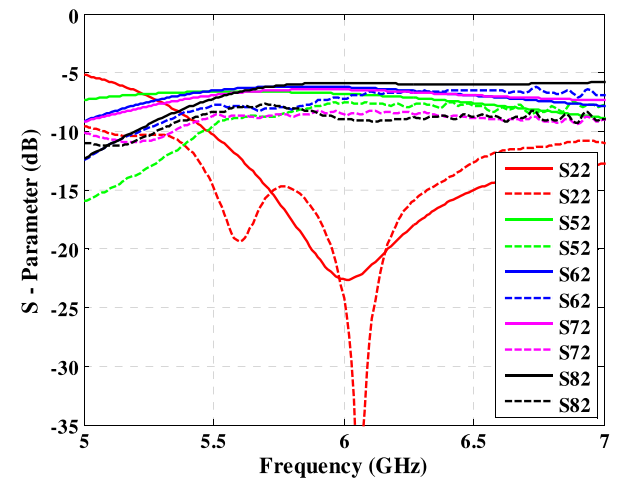
FIGURE 9. Photograph of the fabricated BM under test.

array antenna is obtained in theory from the normalized array factor (AF) given by [26]:

$$AF = \left| \frac{\sin \left(N\pi \frac{d}{\lambda} (\sin \theta - \sin \theta_0) \right)}{N\pi \frac{d}{\lambda} (\sin \theta - \sin \theta_0)} \right| \quad (21)$$



(a)



(b)

FIGURE 10. Measured and simulated radiation pattern of the BM when; (a) port 1 is excited; (b) port 2 is excited.

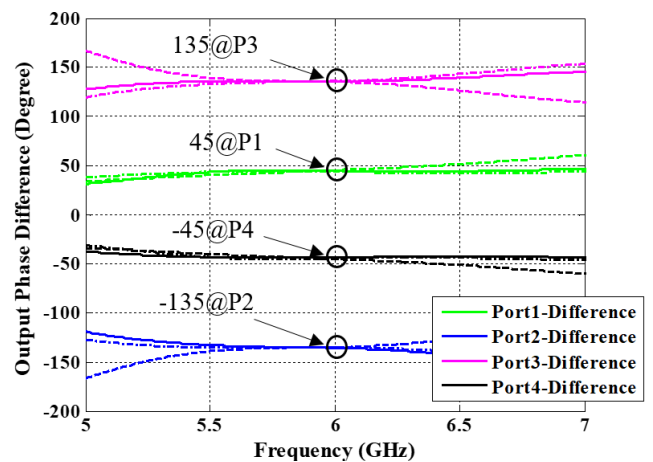


FIGURE 11. Progressive phase differences when each port is excited separately.

where N is the number of antenna elements, d is the distance between adjacent elements of the antenna array, θ_0 is the

beam angle and λ is the propagation wavelength at the free space. The beam angle θ_0 can be obtained from:

$$\theta_0 = \sin^{-1} \left(\frac{\beta \lambda}{2\pi d} \right) \quad (22)$$

where β , is the progressive phase difference of the excitation current within the antenna elements fed by the beam steering network. The distance between the antenna elements is usually taken to be $\lambda/2$. Taking d slightly above or below $\lambda/2$ increases the side lobes in the radiation pattern. The theoretical beam scanned angle, θ_0 and the corresponding phase difference are computed and summarized in Table 3.

TABLE 3. Beam scanned angle and the corresponding phase difference of 4 × 4 Butler matrix.

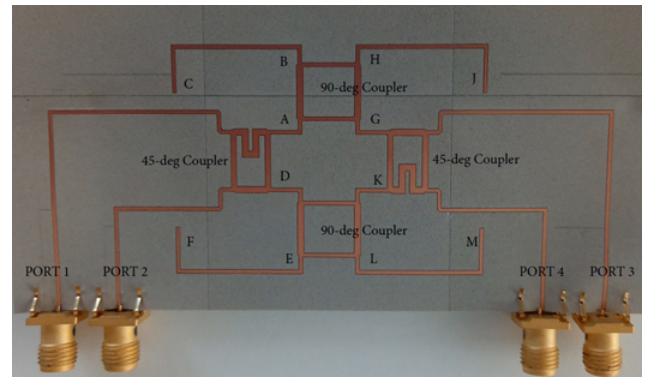
PORT	Progressive Difference β	Phase Angle θ_0	Scanned Beam
#1	+45°	+14.5°	
#2	-135°	-48.1°	
#3	+135°	+48.1°	
#4	-45°	-14.5°	

Even with the good performances exhibited by the proposed BM presented in the previous section, the absolute goal is to feed an antenna array with the BM. Due to the topology of the proposed BM. Traditionally, coaxial cables are sometimes used to convey the energy from the outputs of BM to the inputs of antenna array. In this paper, the antenna array is excited without the use of any cable because of two famous reasons. Firstly, when the lengths of these cables are not the same, there may be a phase mismatch at the output of the BM. Secondly, the cables itself will introduce some losses, which will degrade the performance of the beamforming network.

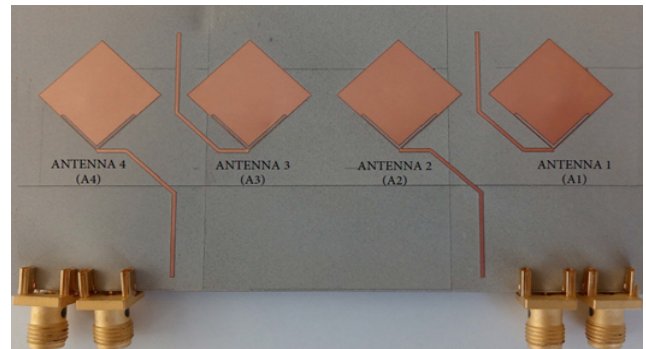
Slots are modeled and used to couple the energy from the top layer of the BM to the bottom layer where the antenna array are placed. This technique has advantage of having a compact solution of BM beamforming network by utilizing the ground plane of the BM to place the antenna array. The photograph of the fabricated BM integrated with linear antenna array is shown in Fig. 12.

When port 1 of the BM is excited, the power travels and divides equally at the output port of the modified coupler referred to as 45° coupler at point 'A' and 'D' with each point at -3 dB. The signal from point 'A' divides into two at the output of hybrid coupler referred to as 90° coupler at point 'B' and 'H' with each point at -3dB. The signal at point 'C' is therefore at -6 dB point. This signal is used to excite antenna 'A1' in Fig. 12 (b). The signal at point 'D' also goes to point 'E' and 'F' and excite antenna 'A2'. This energy is coupled by the principle of electromagnetism to the antenna feed lines to through a slot created at the common ground between the top substrate and the bottom substrate as depicted in Fig. 12.

Similarly, when port 2 of the BM is excited with signal, it divides at points 'A' and 'B'. The signal at point 'A' goes



(a)



(b)

FIGURE 12. Photograph of the proposed BM, (a) top view showing the BM; (b) the linear antenna array excited using slot-coupled technique.

TABLE 4. Performance comparison the proposed BM with related articles.

Ref.	Technique	Return loss	Amplitude imbalance	Phase error	-10 dB Bandwidth
[10]	Microstrip	19 dB	1 dB	0.9°	-
[11]	TF-IPD	13 dB	1.1 dB	13°	8%
[12]	SIW	12 dB	0.4 dB	3°	13.3%
[18]	Multi-layered	25 dB	0.64 dB	2°	6.5%
[19]	CMOS	14 dB	1 dB	12°	8%
[20]	Microstrip	24.1 dB	0.4 dB	0.9°	20.1%
This work	Microstrip	25.6 dB	3 dB	3°	37.1%

to point 'B' then 'C' and excites antenna 'A1'. While the signal at 'B' goes to point 'F' via 'E' and excite antenna 'A2'. The same sequence continued when port 3 and port 4 are separately excited.

The measurements and simulations results of the polar radiation patterns and the cartesian plots are shown in Fig. 13. When power is injected into port 1, the main beam radiates towards +15.3° and when the power is excited to port 2, the main beam angle switches to -47.6°. Similarly, due to symmetry of the BM, when power is excited at port 3 and port 4, similar but beam pattern with opposite sign as those obtained to those in case of port 2 and port 1 respectively.

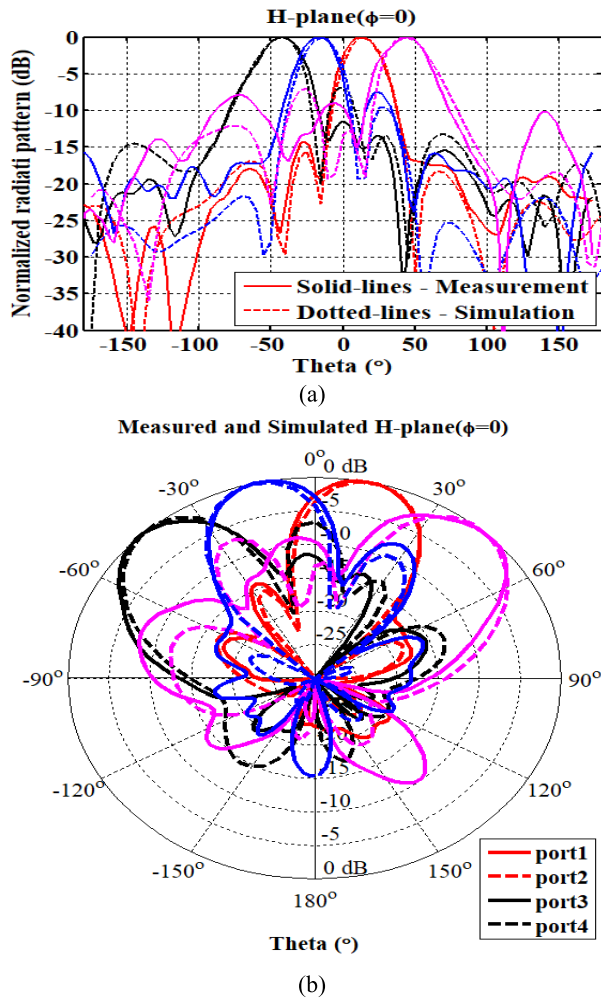


FIGURE 13. Measured and simulated radiation pattern of the BM. (a) cartesian plot; (b) polar plot.

The measured S-parameter results obtained from the proposed BM are compared with other designs as shown in Table 4. It can be seen that; the performance of the proposed design has a return loss better than -25.6 dB at the center frequency. Comparing with other designs, only [18] have comparative return loss to that of the proposed BM. However, in terms of the average phase error, the proposed BM has better performance as compared with [11] and [19]. Bandwidth of the proposed design has better performance than all those in comparison. It can further be observed that, unlike in the other designs in comparison, the proposed design uses a relatively simple microstrip technique for the implementation of the BM.

V. CONCLUSION

This paper presents the design of BM using only couplers. The design was accomplished with the help of a modified hybrid coupler which is capable of outputting 45° phase difference. This coupler replaces the function of a hybrid coupler and the 45° phase shifter in the design of this BM. It exhibits an excellent performance with wideband up to 30.2% and phase imbalance of $45^\circ \pm 5^\circ$ in the whole oper-

ating band. This type of coupler drastically simplifies the design of the BM. The Butler matrix has simple structure and good radiating performance, capable of radiating four slanted beams deposited at $+15.3^\circ$, -48.0° , $+48.0^\circ$, and -15.3° with acceptable measured gain, return losses, transmission coefficients and progressive phase difference. Based on the results obtained, the proposed design will be attractive candidate in the future 5G communication systems.

REFERENCES

- [1] S. Karamzadeh, V. Rafii, M. Kartal, and B. S. Virdee, "Modified circularly polarised beam steering array antenna by utilised broadband coupler and 4 × 4 butler matrix," *IET Microw., Antennas Propag.*, vol. 9, no. 9, pp. 975–981, 2015.
- [2] A. Moscoso-Martir, I. Molina-Fernandez, and A. Ortega-Monux, "Wide-band slot-coupled butler matrix," *IEEE Microw. Wireless Compon. Lett.*, vol. 24, no. 12, pp. 848–850, Dec. 2014.
- [3] K. Wincza, S. Gruszczynski, and K. Sachse, "Broadband planar fully integrated 8 × 8 butler matrix using coupled-line directional couplers," *IEEE Trans. Microw. Theory Techn.*, vol. 59, no. 10, pp. 2441–2446, Oct. 2011.
- [4] K. Staszek, S. Gruszczynski, and K. Wincza, "Broadband measurements of S-parameters utilizing 4 × 4 butler matrices," *IEEE Trans. Microw. Theory Techn.*, vol. 61, no. 4, pp. 1692–1699, Apr. 2013.
- [5] K. Wincza and S. Gruszczynski, "Broadband integrated 8 × 8 butler matrix utilizing quadrature couplers and schiffman phase shifters for multibeam antennas with broadside beam," *IEEE Trans. Microw. Theory Techn.*, vol. 64, no. 8, pp. 2596–2604, Aug. 2016.
- [6] T.-Y. Chin, J.-C. Wu, S.-F. Chang, and C.-C. Chang, "A V-band 8 × 8 CMOS butler matrix MMIC," *IEEE Trans. Microw. Theory Techn.*, vol. 58, no. 12, pp. 3538–3546, Dec. 2010.
- [7] F. Casini, R. V. Gatti, L. Marcaccioli, and R. Sorrentino, "A novel design method for Blass matrix beam-forming networks," in *Proc. Eur. Microw. Conf.*, Oct. 2007, pp. 1511–1514.
- [8] K. Tekkouk, M. Ettorre, L. Le Coq, and R. Sauleau, "Multibeam SIW slotted waveguide antenna system fed by a compact dual-layer Rotman lens," *IEEE Trans. Antennas Propag.*, vol. 64, no. 2, pp. 504–514, Feb. 2016.
- [9] T. Djerfai, N. J. G. Fonseca, and K. Wu, "Planar Ku-band 4 × 4 Nolen matrix in SIW technology," *IEEE Trans. Microw. Theory Techn.*, vol. 58, no. 2, pp. 259–266, Feb. 2010.
- [10] S. A. Babale, S. Lawan, S. K. A. Rahim, and I. O. Stella, "Implimentation of 4 × 4 butler matrix using silver-nono instant inkjet printing technology," in *Proc. IEEE 3rd Int. Conf. Electro-Technol. Nat. Develop.(NIGERCON)*, Owerri, Nigeria, 2017, pp. 514–518.
- [11] Y.-S. Lin and J.-H. Lee, "Miniature Butler matrix design using glass-based thin-film integrated passive device technology for 2.5-GHz applications," *IEEE Trans. Microw. Theory Techn.*, vol. 61, no. 7, pp. 2594–2602, Jul. 2013.
- [12] Q.-L. Yang, Y.-L. Ban, J.-W. Lian, Z.-F. Yu, and B. Wu, "SIW butler matrix with modified hybrid coupler for slot antenna array," *IEEE Access*, vol. 4, pp. 9561–9569, Dec. 2016.
- [13] M. Fakharzadeh, P. Mousavi, S. Safavi-Naeini, and S. H. Jamali, "The effects of imbalanced phase shifters loss on phased array gain," *IEEE Antennas Wireless Propag. Lett.*, vol. 7, pp. 192–196, Feb. 2008.
- [14] S. Y. Zheng, W. S. Chan, and K. F. Man, "Broadband phase shifter using loaded transmission line," *IEEE Microw. Wireless Compon. Lett.*, vol. 20, no. 9, pp. 498–500, Sep. 2010.
- [15] Y.-X. Guo, Z.-Y. Zhang, and L. Ong, "Improved wide-band Schiffman phase shifter," *IEEE Trans. Microw. Theory Techn.*, vol. 54, no. 3, pp. 1196–1200, Mar. 2006.
- [16] L. Markley and G. V. Eleftheriades, "An ultra-compact microstrip crossover inspired by contra-directional even and odd mode propagation," *IEEE Microw. Compon. Lett.*, vol. 24, no. 7, pp. 436–438, Jul. 2014.
- [17] F. Lin, S. W. Wong, and Q.-X. Chu, "Compact design of planar continuously tunable crossover with two-section coupled lines," *IEEE Trans. Microw. Theory Techn.*, vol. 62, no. 3, pp. 408–415, Mar. 2014.
- [18] K. Tekkouk, J. Hirokawa, R. Sauleau, M. Ettorre, M. Sano, and M. Ando, "Dual-layer ridged waveguide slot array fed by a butler matrix with sidelobe control in the 60-GHz band," *IEEE Trans. Antennas Propag.*, vol. 63, no. 9, pp. 3857–3867, Sep. 2015.

- [19] W. Choi, K. Park, Y. Kim, K. Kim, and Y. Kwon, "A V-band switched beam-forming antenna module using absorptive switch integrated with 4×4 butler matrix in $0.13\text{-}\mu\text{m}$ CMOS," *IEEE Trans. Microw. Theory Techn.*, vol. 58, no. 12, pp. 4052–4059, Dec. 2010.
- [20] G. Tian, J.-P. Yang, and W. Wu, "A novel compact butler matrix without phase shifter," *IEEE Microw. Wireless Compon. Lett.*, vol. 24, no. 5, pp. 306–308, May 2014.
- [21] V. F. Fusco and J. A. C. Stewart, "Design and synthesis of patch microwave couplers," in *Proc. 16th Eur. Microw. Conf.*, Sep. 1986, pp. 401–406.
- [22] S. Sun and L. Zhu, "Miniaturised patch hybrid couplers using asymmetrically loaded cross slots," *IET Microw., Antennas Propag.*, vol. 4, no. 9, pp. 1427–1433, Sep. 2010.
- [23] M.-J. Park, "Comments on 'quasi-arbitrary phase-difference hybrid coupler,'" *IEEE Trans. Microw. Theory Techn.*, vol. 61, no. 3, pp. 1725–1727, Apr. 2013.
- [24] D. M. Pozar, *Microwave Engineering*. Hoboken, NJ, USA: Wiley, 2009.
- [25] S. A. Babale, S. K. A. Rahim, M. Jusoh, and L. Zahid, "Branch-line coupler using PDMS and Shieldit Super fabric conductor," *Appl. Phys. A, Solids Surf.*, vol. 123, no. 2, p. 117, Jan. 2017.
- [26] A. B. Constantine, "Antenna theory: Analysis and design," in *Microstrip Antennas*, 3rd ed. Hoboken, NJ, USA: Wiley, 2005.



OUMAR ALASSANE BARRO received the M.Sc. degree in signal processing and telecommunication engineering and the Ph.D. degree in signal processing and telecommunications from the University of Rennes 1, Rennes, France, in 2013 and 2016, respectively. His current research interests include reconfigurable plasma antennas, 3-D antenna technologies, and reconfigurable antennas from microwave-to-millimeter wave frequencies.



MOHAMED HIMDI received the Ph.D. degree in signal processing and telecommunications from the University of Rennes 1, Rennes, France, in 1990. Since 2003, he has been a Professor with the University of Rennes 1. He is currently the Head of the High Frequency and Antenna Department, Institut d'Electronique et Télécommunications de Rennes, Unité Mixte de Recherche, Center National de la Recherche Scientifique. He has authored or co-authored 73 journal papers, over 170 papers in conference proceedings, and two book chapters. He holds 24 patents in the area of antennas. His research activities concern passive and active millimeter-wave antennas. His research interests also include theoretical and applied computational electromagnetics, development of new architectures of printed antenna arrays, and new 3-D antenna technologies. He was a recipient of the 1992 International Symposium on Antennas and Propagation Conference Young Researcher Scientist Fellowship (Japan) and the 1995 Award presented by the International Union of Radio Scientists (Russia). He was a Laureat of the Second National Competition for the Creation of Enterprises in Innovative Technologies in 2000 (Ministry of Industry and Education, France).



SULEIMAN ALIYU BABALE (S'17) received the bachelor's degree in electrical engineering from Bayero University Kano, Nigeria, in 2005, and the M.Sc. degree from Ahmadu Bello University, Zaria, Nigeria, in 2012, the Ph.D. degree in electrical engineering with majors in telecommunications from Universiti Teknologi Malaysia, Johor Bahru, Malaysia, in 2018. He has been a Lecturer with Bayero University Kano since 2009 and a Registered Member of the Council for the Regulation of Engineering in Nigeria since 2011. His main research interests are in millimeter-wave multibeam antenna array with Butler matrix beamforming network for 5G wireless communications.

tion of Engineering in Nigeria since 2011. His main research interests are in millimeter-wave multibeam antenna array with Butler matrix beamforming network for 5G wireless communications.



SHARUL KAMAL ABDUL RAHIM received the degree in electrical engineering from the University of Tennessee, USA, in 1996, the M.Sc. degree in engineering (communication engineering) from Universiti Teknologi Malaysia (UTM) in 2001, and the Ph.D. degree in wireless communication system from the University of Birmingham, U.K., in 2007. He is currently a Professor with the Wireless Communication Centre, Faculty of Electrical Engineering, UTM Skudai. He has published more

than 50 journal papers and technical proceedings on rain attenuations, smart antenna system, microwave design and reconfigurable antenna in national, and international journals and conferences. His research interest is smart antenna on communication system. He is a member of the IEEE Malaysia Section, the Member Board of Engineer Malaysia, the Institute of Engineer Malaysia, and the Eta Kappa Nu Chapter (International Electrical Engineering Honor Society, University of Tennessee).



MOHSEN KHALILY (M'13–SM'18) joined Institute for Communication Systems (ICS), home of 5G Innovation Centre (5GIC) at University of Surrey, U.K., as a research fellow on antenna and propagation, since December 2015. Before joining 5GIC, he worked with Wireless Communication Center (WCC), Universiti Teknologi Malaysia (UTM), as a Senior Lecturer and a Post-Doctoral Research Fellow, from December 2012 to December 2015. Dr. Khalily is an IEEE Senior Member (SMIEEE), a Member of the IEEE Antennas and Propagation Society, IEEE Communication Society, and IEEE Microwave Theory and Techniques Society, an Associate Editor for the IEEE Access, and has published almost 70 academic papers in international peer-reviewed journals and conference proceedings. His research interests include: dielectric resonator antennas, MIMO antennas, phased array antennas, hybrid beamforming, and millimetre-wave antennas and propagation.

...